

Determination of galaxy photometric redshifts using Conditional Generative Adversarial Networks (CGANs)

M. Garcia-Fernandez^{1a}

^aSchool of Architecture, Engineering and Design, Universidad Europea de Madrid, Calle Tajo s/n, Villaviciosa de Odon, 28670, Madrid, Spain

Abstract

Accurate and reliable photometric redshift determination is one of the key aspects for wide-field photometric surveys. Determination of photometric redshift for galaxies, has been traditionally solved by use of machine-learning and artificial intelligence techniques trained on a calibration sample of galaxies, where both photometry and spectrometry are available. On this paper, we present a new algorithmic approach for determining photometric redshifts of galaxies using Conditional Generative Adversarial Networks (CGANs). The proposed implementation is able to determine both point-estimation and probability-density estimations for photometric redshifts. The methodology is tested with data from Dark Energy Survey (DES) Y1 data and compared with other existing algorithm such as a Mixture Density Network (MDN). Although results obtained show a superiority of MDN, CGAN quality-metrics are close to the MDN results, opening the door to the use of CGAN at photometric redshift estimation.

Keywords: Conditional Generative Adversarial Networks, photometric-redshift, galaxy-surveys

1. Introduction

Wide-field photometric surveys have been a major source for experimental results for Observational Cosmology. Among many of the present and future

¹manuel.garcia2@universidadeuropea.es

photometric surveys we can find: DES², LSST³, PAU⁴, J-PAS⁵ and *Euclid*⁶. One of the key aspects of wide-field photometric surveys is the reliable determination of the redshift of the galaxies. At photometric surveys, the redshift of galaxy spectra is inferred by measuring the brightness of galaxies at broad-band filters instead of determining the Doppler shift of their spectra with a high-resolution spectrometer.

The usual approach for translating from the brightness measured at the broad-band filters to a redshift, is the use of machine-learning and artificial intelligence. These techniques, make use of a calibration sample of galaxies with known both the photometry and the high-resolution spectra. This calibration sample, is used by the machine-learning algorithms as a source for indentifying and discovering patterns relating the brightness at the different broad-band filters with the spectroscopic redshift.

Previous machine-learning algorithms for photometric redshift determination have included: neural networks (Collister and Lahav, 2004; Sadeh et al., 2016; Mahmud Pathi et al., 2024; Hoyle, 2016; Chunduri and Mahesh, 2023; Carrasco Kind and Brunner, 2013; Almosallam et al., 2016; Cavioti et al., 2017), boosted decision trees (Gerdes et al., 2010), convolutional neural networks (D’Isanto and Polsterer, 2018; Schuldt et al., 2021), bayesian neural networks (Lima et al., 2022), random forest (Lu et al., 2023), recurrent neural networks (Luo et al., 2024) and nearest neighbours (Graham et al., 2018). A good systematic review on the different types of photometric redshift algorithms can be found at Sánchez et al. (2014); Salvato et al. (2019) and Newman and Gruen (2022). Previous photometric redshift machine-learning algorithms that are capable of producing a probability density estimation for the redshift, instead of a point estimation, include: classification algorithms (Rau et al., 2015), hierarchical-models (Leistedt et al., 2019) and mixture density networks (MDNs) (Ansari, Zoe et al., 2021; Teixeira et al., 2024; D’Isanto, A. and Polsterer, K. L., 2018). Nevertheless, these type of algorithms suffer from the pathological defect that the probability-density produced directly by these algorithms, can not be directly interpreted as the redshift probability-density and need additional re-calibrations (Dey et al.,

²<https://www.darkenergysurvey.org>

³<https://www.lsst.org>

⁴<https://pausurvey.org>

⁵<https://www.j-pas.org>

⁶<https://www.euclid-ec.org>

2021).

A new class of neural network that has still not been explored at photometric redshift estimation are the Generative Adversarial Networks (GANs). GANs (Goodfellow et al., 2014), are a set of two neural networks, a Generator network and a Discriminator network that compete between each other. The Generator aims to generate synthetic data mimicking the real data, whereas the Discriminator network aims to identify if a given data-record is synthetic data produced by the Generator or is an observation of the real data. On the process of training this algorithm, both Generator and Discriminator compete with each other in a zero-sum competitive game approach, that is finished when the Generator can completely fool the Discriminator, so the Discriminator is not able to properly disentangle synthetic data from real data. As a consequence of this, the Generator network can accurately map the full probability distribution of the underlying data without the need of providing any prior assumption or template.

A very relevant special case for GANs, are the Conditional Generative Adversarial Networks (CGANs), which instead of tracing the full probability density function of the underlying data, they trace the conditional probability density function, provided some input condition (Mirza and Osindero, 2014).

On this paper, we propose the use of CGANs for estimating photometric redshifts using the magnitudes measured at broad-band filters. This algorithm is tested with data from the Dark Energy Survey Y1 data that is overlapping with SDSS Stripe-82. Results obtained by proposed CGAN are compared with a Mixture Density Network (MDN).

2. Methodology

2.1. Conditional Generative Adversarial Network

Let \mathbf{x}_i be a sample of photometric data from magnitudes measured at broad-band pass filters for the i -th galaxy of some data and y_i its corresponding known spectroscopic redshift, such that $\{(\mathbf{x}_i, y_i)\}_{i=1}^{N_{train}}$ constitutes the data training set. Let \mathbf{z}_i be a vector of randomly-generated numbers⁷, associated to the i th galaxy.

⁷Beware that Computer Science standard notation at literature on GANs, name the random vectors with z . Do not confuse this z with the redshift of the galaxies (that will be either denoted in this paper as y or \hat{y} for spectroscopic or photometric redshifts respectively).

The generator network G constitutes a function such that $\hat{y}_i = G(\mathbf{z}_i|\mathbf{x}_i; \theta_G)$, where \hat{y}_i is the estimated photometric redshift for the set of magnitudes \mathbf{x}_i and θ_G are the weights defining the generator neural network. On the other side, the discriminator network D provides a function such that $p_i = D(\hat{y}_i; \theta_D)$ -with $p_i \in [0, 1]$ - is a classifier that identifies if \hat{y}_i is a real data from the training sample or a synthetic-generated data produced by the generator network and θ_D are the weights defining the discriminator network.

The process of training a GAN network constitutes a min-max problem such that $\min_{\theta_G} \max_{\theta_D} V(D, G)$. The choice of the function $V(D, G)$ is a vast problem within the field of Computer Science. As demonstrated by [Nowozin et al. \(2016\)](#), any GAN can be interpreted as a special type of variational divergence estimation. Thus, the function $V(G, D)$ can be placed on the most generic formulation as

$$V(D, G) = \mathbb{E}_{\mathbf{x} \sim p_d(\mathbf{x})} [\mathbb{E}_{y \sim p_d(y)} [g_f(D(y|\mathbf{x}))]] + \mathbb{E}_{\mathbf{z} \sim p_z(\mathbf{z})} [-f^*(g_f(D(G(\mathbf{z}|\mathbf{x}))))], \quad (1)$$

where g_f denotes the output activation function and f^* is the corresponding Fenchel conjugate function of g_f ([Hiriart-Urruty and Lemaréchal, 2001](#)). The functions g_f and f^* can be chosen freely, provided they are derived from any f -divergence ([Csiszár and Shields, 2004](#); [Liese and Vajda, 2006](#); [Nguyen et al., 2007](#); [Reid and Williamson, 2011](#)). On the other side, $\mathbb{E}_{\mathbf{x} \sim p_d(\mathbf{x})}$, $\mathbb{E}_{y \sim p_d(y)}$ and $\mathbb{E}_{\mathbf{z} \sim p_d(\mathbf{z})}$ denote the expected values over \mathbf{x} , y and \mathbf{z} respectively.

Taking this into account, the loss function to be minimized for the discriminator network is given by

$$\mathcal{L}_D(\theta_D) = \frac{-1}{N_{batch}} \sum_{i=1}^{N_{batch}} [g_f(D(y_i|\mathbf{x}_i; \theta_D)) - f^*(g_f(D(G(\mathbf{z}_i|\mathbf{x}_i); \theta_G)|\mathbf{x}_i; \theta_D))], \quad (2)$$

whereas the loss for the generator to be minimized simultaneously is given by

$$\mathcal{L}_G(\theta_G) = \frac{-1}{N_{batch}} \sum_{i=1}^{N_{batch}} g_f(D(G(\mathbf{z}_i|\mathbf{x}_i; \theta_G)|\mathbf{x}_i; \theta_D)). \quad (3)$$

From all the possible f -divergences, we select the Kullback-Leibler divergence ([Kullback and Leibler, 1951](#)), given by

$$D_{KL}(P, Q) = \int P(\mathbf{x}) \ln \left[\frac{P(\mathbf{x})}{Q(\mathbf{x})} \right] d\mathbf{x}. \quad (4)$$

Thus, by using the KL-divergence as the proposed f -divergence, the corresponding $g_f(x)$ and $g(f^*(x))$ are given by [Nowozin et al. \(2016\)](#)

$$g_f(x) = x \tag{5}$$

and

$$f^*(g_f(x)) = e^{x-1}. \tag{6}$$

By using this f -divergence approach, the photometric redshift inferred by the generator network -given a fixed set of values for the magnitudes \mathbf{x}_i -, will be a function of the random vector \mathbf{z}_j such that

$$\hat{y}_i(\mathbf{z}_j) = G(\mathbf{z}_j|\mathbf{x}_i). \tag{7}$$

Proposed topology of the neural network for the generator is a sequence of 3 fully connected layers, where the first two layers are followed by a Batch Normalization layer and a ReLU activation function. Input neurons of the first fully connected layer has $4 + Z_{DIM}$ neurons with G_{DIM} output neurons. Hidden fully connected layer consist of G_{DIM} input neurons and G_{DIM} output neurons. Final fully connected layer consist of G_{DIM} input neurons and a single output neuron. The input of the generator network is composed by the vector \mathbf{x} of the four galaxy magnitudes and the random vector \mathbf{z} . The output of the generator network is directly the inferred photometric redshift \hat{y} .

The discriminator neural network, is a sequence of 3 fully connected layers, where the first two layers are followed by a Batch Normalization layer and a ReLU activation function. Input neurons of the first fully connected layer has 5 neurons with D_{DIM} output neurons. Hidden fully connected layer consist of D_{DIM} input neurons and D_{DIM} output neurons. Final fully connected layer consist of D_{DIM} input neurons and a single output neuron followed by a sigmoid activation function, $\sigma(x) = 1/(1 + e^{-x})$. The input of the discriminator network is composed by a redshift (spectroscopic $-y$ - or photometric $-\hat{y}$ -), and the vector \mathbf{x} of galaxy magnitudes. The output of the discriminator network is a decimal number between 0 and 1 that indicates the probability of the input galaxy to be real.

Topology of generator and discriminator neural networks can be seen at [Figure 1](#) and a diagram illustrating how the Generator and Discriminator networks interact, can be seen at [Figure 2](#).

More recent works on GANs, have made extensively use of Wasserstein [Arjovsky et al. \(2017\)](#) formalism (WGANs) instead of f -divergences, showing

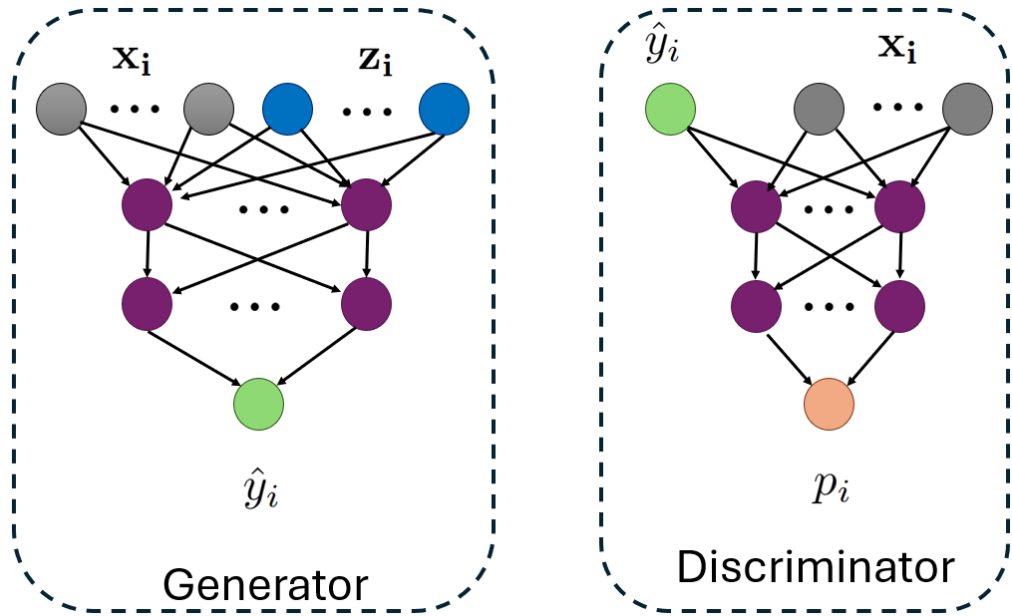


Figure 1: Topology of the Generator and Discriminator networks of the CGAN model. Gray neurons \mathbf{x}_i , denote the input feature vector containing the four MAG_AUTO magnitudes. Blue neurons indicate the Z_{DIM} neurons relative to the input random vector \mathbf{z}_i . Green neuron \hat{y}_i indicate the predicted photometric redshift, which is both the output of the Generator and part of the input of the Discriminator. The orange neuron p_i is the probability of some observation to be synthetic data generated by the Generator or data from the real sample. Purple neurons are the G_{DIM} and D_{DIM} of the hidden layers.

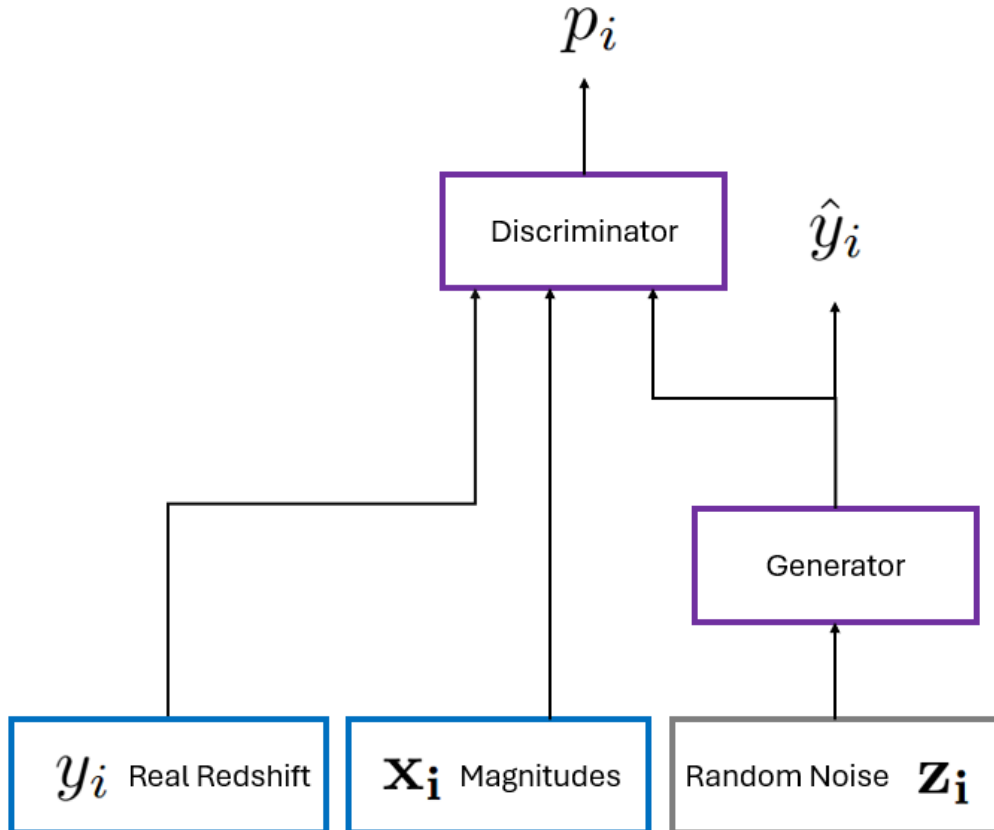


Figure 2: Interaction of the Generator and Discriminator networks of the CGAN approach. A tensor of random noise z_i (gray box) is fed into the Generator network, producing an estimation of the photometric redshift. Tensors containing real spectroscopic redshift (y_i) and the estimated photometric redshifts (\hat{y}_i) are fed into the Discriminator network, which tries to guess which records are real spectroscopic data and which records are produced by the Generator network given the magnitude data x_i (blue box).

superior empirical performance and easier convergence of GANs (Brock et al., 2019; Karras et al., 2018). Nevertheless, WGANs prevent the interpretation of the outputs as a probability density (Song and Ermon, 2020). Thus, Wasserstein formalism has been discarded for this work.

2.2. Mixture Density Network

Mixture Density Networks (MDNs), are a type of machine-learning model that combines a neural-network and a parametric mixture model (Bishop, 1994; McLachlan et al., 2019; Yu et al., 2012). Thus, instead of producing a point estimation, MDNs learn the conditional probability as a linear combination of a finite set of individual probability distributions. To do so, the neural-network of the MDN aims the prediction of the parameters that characterizes the probability distributions and the mixing coefficients. The most common probability density used, is a Gaussian. Thus, the neural network aims to determine the set of parameters $\{(\mu_i, \sigma_i, \pi_i)\}_{i=0}^{N_g}$, where μ_i is the mean of the Gaussian, σ_i the standard-deviation and π_i the mixing coefficients (such that $\sum_{i=0}^{N_g} \pi_i = 1$). On the other side, N_g is the number of gaussians on the mix and shall be a configuration parameter of the model that must be fixed.

In order to compare with a Mixture Density Network, in this work, we will be using the MDN proposal from Ansari, Zoe et al. (2021), where we took the code from companion GitHub⁸ and ported it from Keras to PyTorch. Configuration parameters of the MDN model are kept the same as the original formulation, except the number of neurons of the input layer -where in this work 4 neurons are used instead of the original 22 input neurons-. This is made in order to adapt original Ansari, Zoe et al. (2021) code to the 4 magnitude features of this dataset, instead of the 22 magnitude features used originally at the paper. Thus, MDN model is composed by 30 mixture Gaussians, one input fully-connected layer of 4 neurons and a hidden fully-connected layer of 22 neurons.

3. Data Analysis

Proposed CGAN was tested at DES-Y1 data spectroscopy-matched with SDSS galaxies. Data was taken from the public data releases DR1 (Ab-

⁸<https://github.com/ZoeAnsari/MixtureModelsForPhotometricRedshifts>

bott et al., 2018; Drlica-Wagner et al., 2018) from The Dark Energy Survey Collaboration that are available at the NCSA repository⁹.

Code for the CGAN was implemented under Python¹⁰ using PyTorch¹¹ (Paszke et al., 2019). Full code of this analysis can be found at author’s GitHub repository¹².

From the DES-Y1 proposed sample, we take the Stripe-82 subset of galaxies with matched spectroscopic redshift from SDSS. For consideration of the sample, we restrict ourselves to the galaxies with spectroscopic redshift $0.0 < z_{sp} < 0.8$. This quality cut is imposed to avoid a very long tail up to redshift 2, but with a few galaxies, as the inclusion of these elements on the training sample of the algorithm can potentially introduce biases due to the neural network infer magnitude-redshift relationships from an under-represented sample of galaxies of high-redshift. Selected measurements of magnitudes for the galaxies are the MAG_AUTO magnitudes at the *griz* band-pass filters as measured by SExtractor (Bertin and Arnouts, 1996). The distribution of the *griz* magnitudes and spectroscopic redshift of the selected calibration sample of galaxies can be seen along with their correlation plots at Figure 3. Total number of galaxies at the final calibration sample is 33410. From this final calibration sample, we do a split between a training sample and a test sample with 80% and 20% of the galaxies respectively. The training sample is used for determining the parameters of the photometric redshift algorithm during the training process. On the other side, the test sample is used for measuring the properties of the algorithm on a set of galaxies unseen by the photometric redshift algorithm.

Hyperparameters of the model defining the sizes of the dense layers of generator (G_{DIM}) and the discriminator (D_{DIM}) along with the size the random vector (Z_{DIM}) can be seen at Table 1. Training strategy used the Adam optimizer with an initial learning rate parameter of $lr = 10^{-4}$ for both generator and discriminator network using 10000 training epochs, using a step learning-rate approach reducing the learning rate by a factor of 0.2 every 2000 training epochs. Training strategy is the same for the generator and the discriminator networks. The loss for both generator and discriminator as a function of the training epoch can be seen at Figure 4, showing a good

⁹<https://des.ncsa.illinois.edu/releases/y1a1>

¹⁰<https://www.python.org>

¹¹<https://pytorch.org>

¹²<https://github.com/mgarciafernandez-uem/CGAN-photoz>

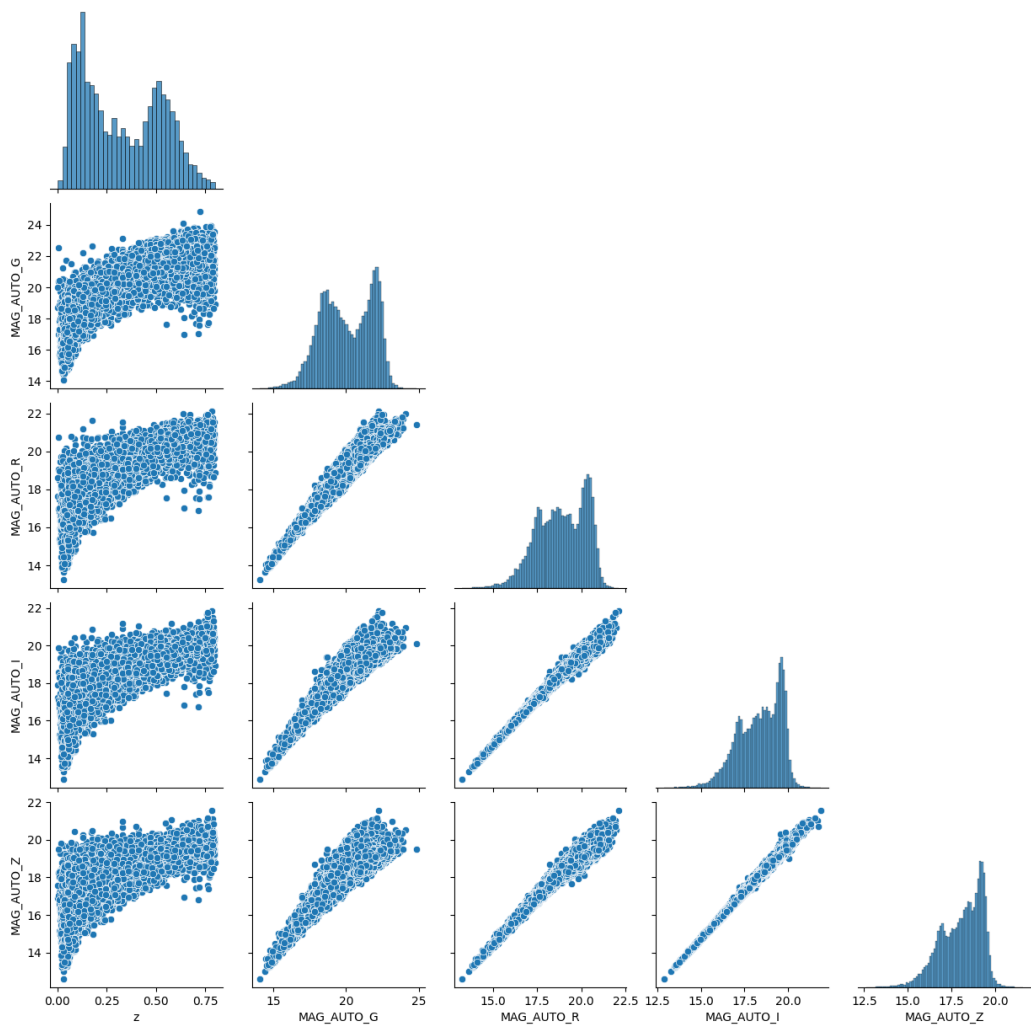


Figure 3: Distribution and correlation of the *griz* MAG_AUTO magnitudes and the measured spectroscopic redshift

Hyperparameter	Value
Z_{DIM}	20
D_{DIM}	32
G_{DIM}	32

Table 1: Hyperparameters of the CGAN used for this paper.

and stable convergence of the losses for both the generator and discriminator networks.

MDN training process involves 5000 training epochs with an initial learning-rate of $lr = 10^{-4}$. Losses and mean-square-error (MSE) for the MDN can be seen at [Figure 5](#)

A comparison of the dispersion between the true spectroscopic redshift and the inferred photometric redshift can be see at [Figure 6](#). From these plots, we can see that the photometric redshifts inferred by the proposed CGAN approach and the MDN can accurately trace the true spectroscopic redshift distribution of the test sample of galaxies.

For determining the quality metric both for point-estimation and probability density estimation, we use the approach from [Teixeira et al. \(2024\)](#), where these metrics are all determined over the test sample of galaxies which have not been seen neither by the CGAN neither the MDN.

3.1. Point-estimation quality metrics

Point-estimation quality metrics involve: the mean absolute bias ($|\bar{\Delta z}|$), the Normalized Median Absolute Deviation (σ_{NMAD}) and the outliers ratio η . Metrics are computed in 20 spectroscopic redshift at the interval $0 \leq z_{sp} \leq 0.8$.

The Normalized Median Absolute Deviation is given by

$$\sigma_{NMAD} = 1.48 \times \text{median} \left(\frac{\Delta z - \text{median}(\Delta z)}{1 + z} \right), \quad (8)$$

whereas the outlier ratio (η) is defined as the ratio of galaxies with

$$\left| \frac{\Delta z}{1 + z} \right| > 0.15. \quad (9)$$

The confidence intervals for these metrics are computed at the 95% confidence level by using bootstrapping. Bootstrapping is implemented by building 1000 samples of the test dataset with each sub-sample having the same

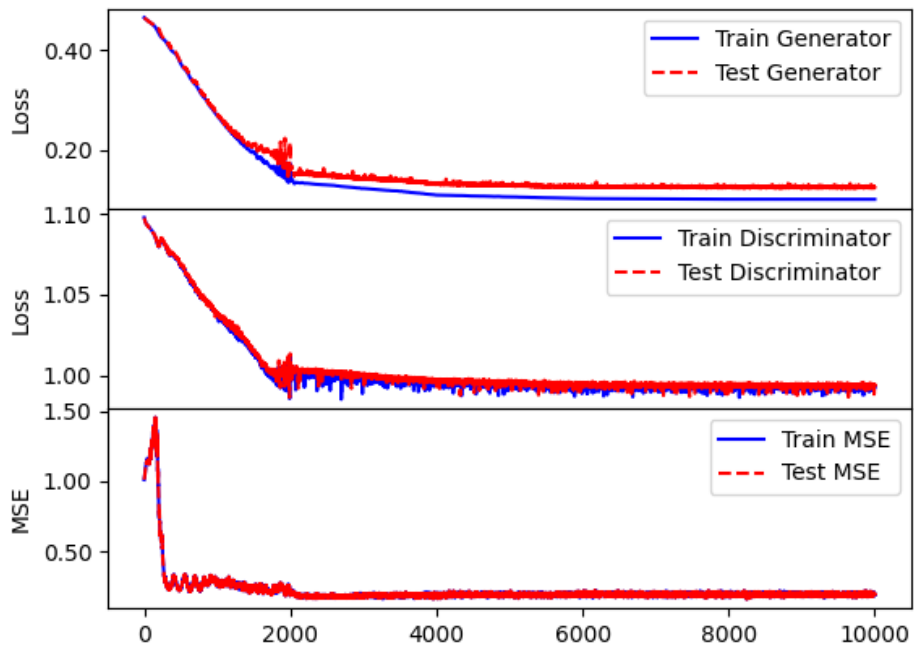


Figure 4: Loss function for the generator and discriminator networks as a function of the training epoch as measured at the training and test data samples. Values of the measured losses have been shifted +1 in order to avoid negative values at the Y-axis. A plot showing the Mean Square Error (MSE) between the inferred photometric redshift and the true spectroscopic redshift is also displayed.

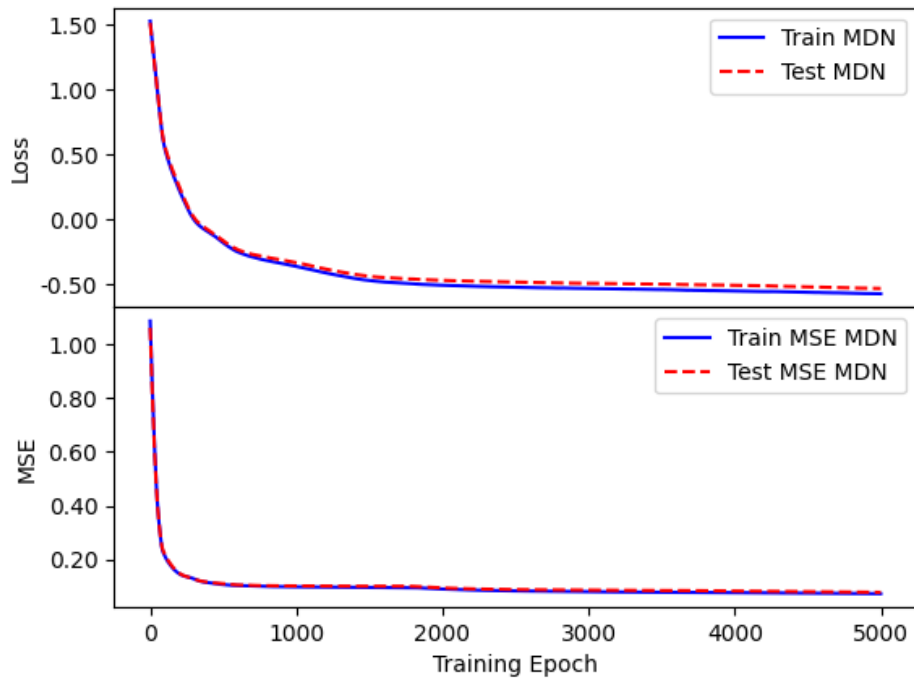


Figure 5: Losses and mean-square-error (MSE), for the Mixture Density Network (MDN).

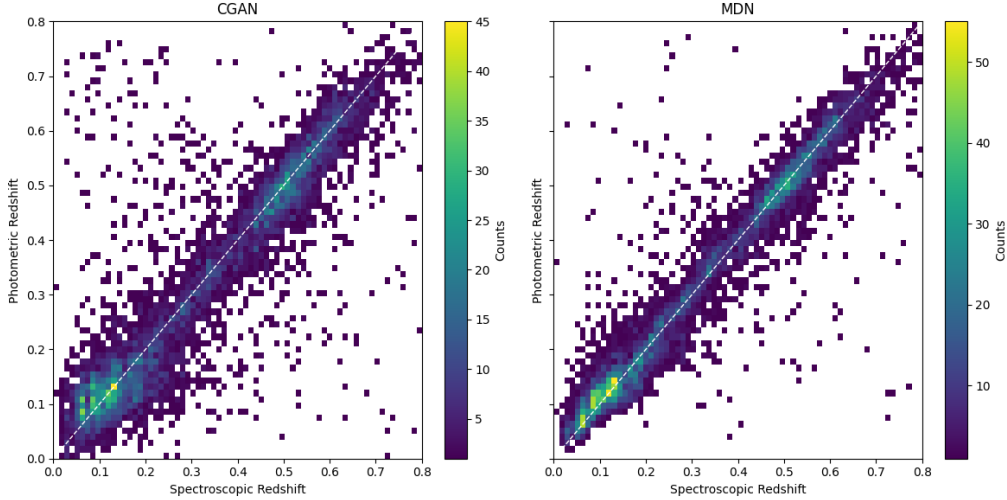


Figure 6: Comparison of the photometric redshift of galaxies and the spectroscopic redshift. Distributions are displayed for proposed Conditional Generative Adversarial Network (CGAN) approach and the Mixture Density Network (MDN). White-dashed line is an eye-guide for the identity.

number of galaxies as in the full test dataset, where each sample is generated by picking randomly with replacement galaxies from the test dataset. Thus, for each subsample at the bootstrap, each point-estimation quality-metric is computed. Then, this set of 1000 metrics is used to determine the respective 2.5% and 97.5% quantiles, which stand for the lower and upper edges of the confidence intervals.

Graphics for these quality metrics can be seen at [Figure 7](#), from which we can see that both CGAN and MDN models have a close performance at quality metrics, being the MDN more accurate than the CGAN, being the latter more prone to outliers.

3.2. Probability-density-function quality metrics

Given a galaxy with spectroscopic redshift z_{sp} , photometric redshift z_{ph} with associated PDF $\phi(z)$, its PIT is defined as ([Dawid, 1984](#); [Lima et al., 2022](#); [Polsterer et al., 2016](#))

$$PIT = \int_{-\infty}^{z_{sp}} \phi(z) dz. \quad (10)$$

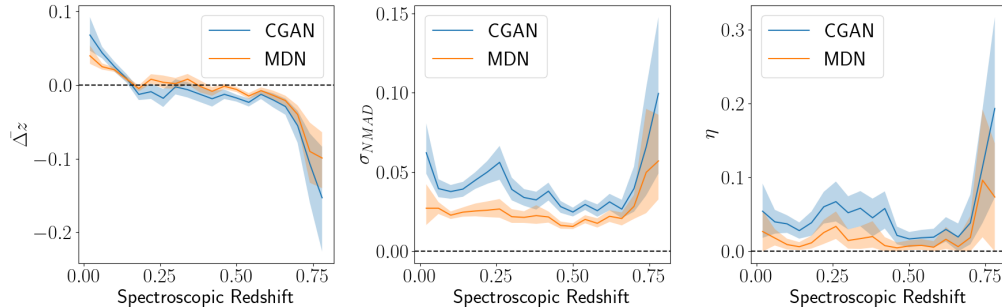


Figure 7: Point-estimation quality-metrics comparison for CGAN and MDN. Left, shows the mean absolute bias $|\bar{\Delta z}|$. Center shows the σ_{NMAD} . Right shows the ratio of outliers η . Solid line stands for the mean value per redshift bin. Shaded area stands for the 95% confidence interval for that redshift bin. Confidence intervals are computed using bootstrap.

As stated by [Mucesh et al. \(2021\)](#), a properly calibrated PDF, will produce an uniform distribution of PIT values for a large sample of galaxies.

The Odds ([Lima et al., 2022](#)) for a galaxy with PDF $\phi(z)$, with photometric redshift z_{ph} is defined as

$$Odds = \int_{z_{ph}-\xi}^{z_{ph}+\xi} \phi(z) dz, \quad (11)$$

where $\xi \in \mathbb{R}$ is a constant parameter that must be fixed before-hand, that is fixed to $\xi = 0.06$ taking the same value as [Teixeira et al. \(2024\)](#). A distribution of Odds peaked towards large values, indicates that the PDF produced are narrow and the inferred photometric redshift is around the most probable value, indicating a reliable PDF. On the other side, low Odds value, indicates that PDFs are broad.

Coverage-Test ([Dalmasso et al., 2020](#); [Hermans et al., 2020](#)), is computed by taking for each galaxy its spectroscopic redshift (z_{sp}) and the PDF ($\phi(z)$). For a prefixed value of confidence level $\alpha - 1$, the edges z_l, z_u of the symmetric interval enclosing a probability of $1 - \alpha$ is computed by using

$$\frac{\alpha}{2} = \int_{-\infty}^{z_l} \phi(z) dz = \int_{z_u}^{\infty} \phi(z) dz. \quad (12)$$

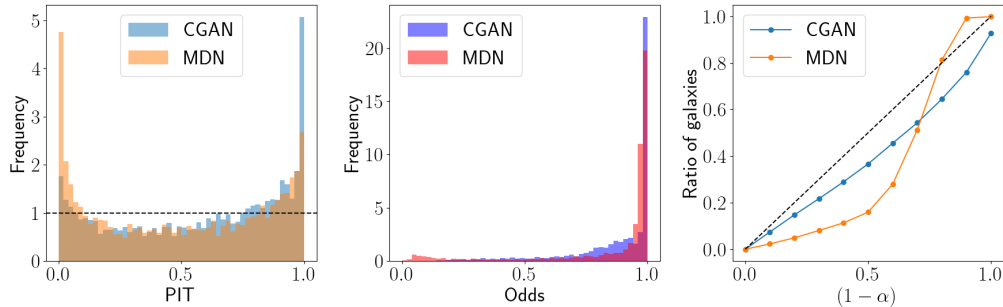


Figure 8: Probability density quality metrics comparison for CGAN and MDN. Left shows the PIT. Center shows the Odds. Right shows the credibility-diagram.

Thus, the ratio of galaxies with spectroscopic redshift z_{sp} at the interval such that $z_l \leq z_{sp} \leq z_u$, must be exactly equal to $1 - \alpha$. A ratio of galaxies within the interval lower than expected, indicates that the PDFs produced are narrower than expected pointing an overconfidence of the algorithm on the determination of the PDFs for the galaxies. On the other side, higher ratios of galaxies than expected, indicate a broader PDFs than expected, pointing a underconfidence of on the determination of the PDFs.

Graphics for these quality-metrics can be found at [Figure 8](#). We can see that both the PIT and Odds distributions of the CGAN and the MDN approaches are very similar. On the other side, we can see on the Coverage-Test, that the measured confidence values for the CGAN, show that both probability densities are skewed towards overconfidence.

In addition, in order to test the capacity of the algorithm to recover the probability density function, the distribution of the spectroscopic redshift of the galaxies is compared with the distribution computed by stacking all the probability densities of the individual galaxies produced by both algorithms. The result can be seen at [Figure 9](#), where we can see that the stacking of the probability densities show a similar description of the underlying data distribution, with the MDN being more closer to spectroscopic data than the CGAN.

4. Conclusions

On this paper, it was presented a new machine-learning technique for photometric redshift estimation using a Conditional Generative Adversarial

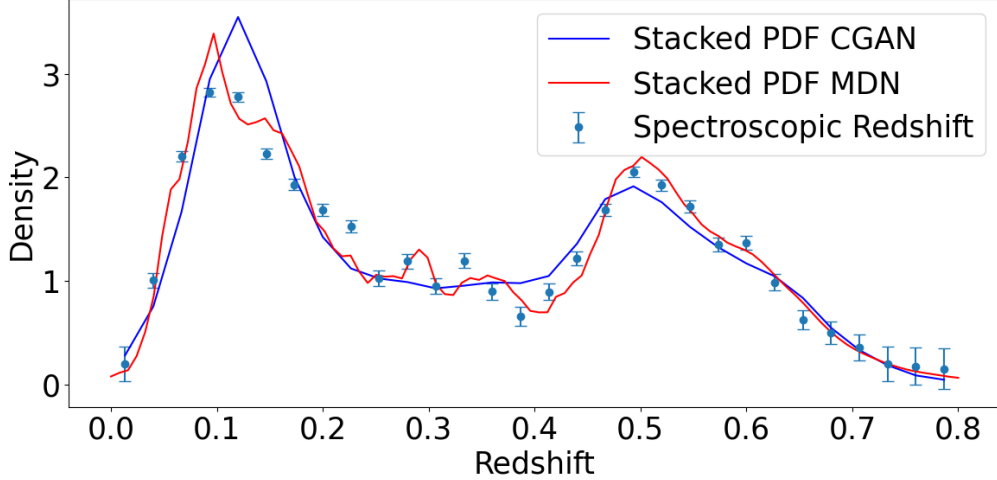


Figure 9: Comparison of the probability density of the spectroscopic redshift with the probability density inferred from the stacking of the probability densities of individual galaxies for CGAN and MDN algorithms.

Network (CGAN). Proposed CGAN technique was tested using Dark Energy Survey Y1 data and compared with a Mixture Density Network (MDN).

Both point-estimation and probability-density quality-metrics indicate CGAN performance is close to the MDN algorithm. Although these metrics clearly demonstrate that MDN performs better than the proposed CGAN, this work constitutes a proof of concept indicating that the use of CGAN with the f -divergence formalism is an algorithm that can be used for photometric redshift determination, opening the door to further developments on the use of CGANs at this field.

Future work will explore the possibility of including a finer selection by population of galaxies (main-sequence, LRGs, etc.) that can be included as an additional parameter of the CGAN that shall be computed as a previous step to the photometric redshift CGAN.

Acknowledgments

Author wants to thank to Departamento de Computación y Tecnología of Universidad Europea de Madrid for providing access to computing resources at the LORCA Cluster.

References

Abbott, T.M.C., Abdalla, F.B., Allam, S., Amara, A., Annis, J., Asorey, J., Avila, S., Ballester, O., Banerji, M., Barkhouse, W., Baruah, L., Baumer, M., Bechtol, K., Becker, M.R., Benoit-Lévy, A., Bernstein, G.M., Bertin, E., Blazek, J., Bocquet, S., Brooks, D., Brout, D., Buckley-Geer, E., Burke, D.L., Busti, V., Campisano, R., Cardiel-Sas, L., Carnero Rosell, A., Carrasco Kind, M., Carretero, J., Castander, F.J., Cawthon, R., Chang, C., Chen, X., Conselice, C., Costa, G., Crocce, M., Cunha, C.E., D'Andrea, C.B., da Costa, L.N., Das, R., Daues, G., Davis, T.M., Davis, C., De Vicente, J., DePoy, D.L., DeRose, J., Desai, S., Diehl, H.T., Dietrich, J.P., Dodelson, S., Doel, P., Drlica-Wagner, A., Eifler, T.F., Elliott, A.E., Evrard, A.E., Farahi, A., Fausti Neto, A., Fernandez, E., Finley, D.A., Flaugher, B., Foley, R.J., Fosalba, P., Friedel, D.N., Frieman, J., García-Bellido, J., Gaztanaga, E., Gerdes, D.W., Giannantonio, T., Gill, M.S.S., Glazebrook, K., Goldstein, D.A., Gower, M., Gruen, D., Gruendl, R.A., Gschwend, J., Gupta, R.R., Gutierrez, G., Hamilton, S., Hartley, W.G., Hinton, S.R., Hislop, J.M., Hollowood, D., Honscheid, K., Hoyle, B., Huterer, D., Jain, B., James, D.J., Jeltama, T., Johnson, M.W.G., Johnson, M.D., Kacprzak, T., Kent, S., Khullar, G., Klein, M., Kovacs, A., Koziol, A.M.G., Krause, E., Kremin, A., Kron, R., Kuehn, K., Kuhlmann, S., Kuropatkin, N., Lahav, O., Lasker, J., Li, T.S., Li, R.T., Liddle, A.R., Lima, M., Lin, H., López-Reyes, P., MacCrann, N., Maia, M.A.G., Maloney, J.D., Manera, M., March, M., Marriner, J., Marshall, J.L., Martini, P., McClintock, T., McKay, T., McMahan, R.G., Melchior, P., Menanteau, F., Miller, C.J., Miquel, R., Mohr, J.J., Morganson, E., Mould, J., Neilsen, E., Nichol, R.C., Nogueira, F., Nord, B., Nugent, P., Nunes, L., Ogando, R.L.C., Old, L., Pace, A.B., Palmese, A., Paz-Chinchón, F., Peiris, H.V., Percival, W.J., Petravick, D., Plazas, A.A., Poh, J., Pond, C., Porredon, A., Pujol, A., Refregier, A., Reil, K., Ricker, P.M., Rollins, R.P., Romer, A.K., Roodman, A., Rooney, P., Ross, A.J., Rykoff, E.S., Sako, M., Sanchez, M.L., Sanchez, E., Santiago, B., Saro, A., Scarpine, V., Scolnic, D., Serrano, S., Sevilla-Noarbe, I., Sheldon, E., Shipp, N., Silveira, M.L., Smith, M., Smith, R.C., Smith, J.A., Soares-Santos, M., Sobreira, F., Song, J., Stebbins, A., Suchyta, E., Sullivan, M., Swanson, M.E.C., Tarle, G., Thaler, J., Thomas, D., Thomas, R.C., Troxel, M.A., Tucker, D.L., Vikram, V., Vivas, A.K., Walker, A.R., Wechsler, R.H., Weller, J., Wester, W., Wolf, R.C., Wu, H., Yanny, B., Zenteno, A., Zhang, Y., Zuntz,

- J., DES Collaboration, Juneau, S., Fitzpatrick, M., Nikutta, R., 2018. The Dark Energy Survey: Data Release 1. *Astrophysical Journal, Supplement* 239, 18. doi:[10.3847/1538-4365/aae9f0](https://doi.org/10.3847/1538-4365/aae9f0), [arXiv:1801.03181](https://arxiv.org/abs/1801.03181).
- Almosallam, I.A., Jarvis, M.J., Roberts, S.J., 2016. GPZ: non-stationary sparse Gaussian processes for heteroscedastic uncertainty estimation in photometric redshifts. *Monthly Notices of the Royal Astronomical Society* 462, 726–739. doi:[10.1093/mnras/stw1618](https://doi.org/10.1093/mnras/stw1618), [arXiv:1604.03593](https://arxiv.org/abs/1604.03593).
- Ansari, Zoe, Agnello, Adriano, Gall, Christa, 2021. Mixture models for photometric redshifts. *A&A* 650, A90. URL: <https://doi.org/10.1051/0004-6361/202039675>, doi:[10.1051/0004-6361/202039675](https://doi.org/10.1051/0004-6361/202039675).
- Arjovsky, M., Chintala, S., Bottou, L., 2017. Wasserstein generative adversarial networks, in: Precup, D., Teh, Y.W. (Eds.), *Proceedings of the 34th International Conference on Machine Learning*, PMLR. pp. 214–223. URL: <https://proceedings.mlr.press/v70/arjovsky17a.html>.
- Arnouts, S., Ilbert, O., 2011. LePHARE: Photometric Analysis for Redshift Estimate. *Astrophysics Source Code Library*, record ascl:1108.009.
- Benítez, N., 2011. BPZ: Bayesian Photometric Redshift Code. *Astrophysics Source Code Library*, record ascl:1108.011.
- Bertin, E., Arnouts, S., 1996. SExtractor: Software for source extraction. *Astronomy and Astrophysics, Supplement* 117, 393–404. doi:[10.1051/aas:1996164](https://doi.org/10.1051/aas:1996164).
- Bishop, C.M., 1994. Mixture density networks. URL: <https://api.semanticscholar.org/CorpusID:118227751>.
- Bishop, C.M., 2006. *Pattern Recognition and Machine Learning*. Information Science and Statistics, Springer.
- Bolzonella, M., Miralles, J.M., Pelló, R., 2011. Hyperz: Photometric Redshift Code. *Astrophysics Source Code Library*, record ascl:1108.010.
- Breiman, L., 2001. Random forests. *Machine Learning* 45, 5–32. URL: <https://doi.org/10.1023/A:1010933404324>, doi:[10.1023/A:1010933404324](https://doi.org/10.1023/A:1010933404324).

- Brock, A., Donahue, J., Simonyan, K., 2019. Large scale GAN training for high fidelity natural image synthesis, in: International Conference on Learning Representations. URL: <https://openreview.net/forum?id=B1xsqj09Fm>.
- Canavos, G.C., Urbina Medal, E.G., Valencia Ramírez, G.J., 1988. Probabilidad y estadística : aplicaciones y métodos. McGraw-Hill/ Interamericana de México, México [etc.
- Carrasco Kind, M., Brunner, R.J., 2013. TPZ: photometric redshift PDFs and ancillary information by using prediction trees and random forests. Monthly Notices of the Royal Astronomical Society 432, 1483–1501. doi:[10.1093/mnras/stt574](https://doi.org/10.1093/mnras/stt574), [arXiv:1303.7269](https://arxiv.org/abs/1303.7269).
- Cavuoti, S., Amaro, V., Brescia, M., Vellucci, C., Tortora, C., Longo, G., 2017. METAPHOR: a machine-learning-based method for the probability density estimation of photometric redshifts. Monthly Notices of the Royal Astronomical Society 465, 1959–1973. doi:[10.1093/mnras/stw2930](https://doi.org/10.1093/mnras/stw2930), [arXiv:1611.02162](https://arxiv.org/abs/1611.02162).
- Chang, C.C., Lin, C.J., 2011. Libsvm: A library for support vector machines. ACM Trans. Intell. Syst. Technol. 2. URL: <https://doi.org/10.1145/1961189.1961199>, doi:[10.1145/1961189.1961199](https://doi.org/10.1145/1961189.1961199).
- Chunduri, K., Mahesh, M., 2023. Deep Learning Approach to Photometric Redshift Estimation. arXiv e-prints , arXiv:2310.16304doi:[10.48550/arXiv.2310.16304](https://doi.org/10.48550/arXiv.2310.16304), [arXiv:2310.16304](https://arxiv.org/abs/2310.16304).
- Coe, D., Benítez, N., Sánchez, S.F., Jee, M., Bouwens, R., Ford, H., 2006. Galaxies in the hubble ultra deep field. i. detection, multiband photometry, photometric redshifts, and morphology. The Astronomical Journal 132, 926. URL: <https://dx.doi.org/10.1086/505530>, doi:[10.1086/505530](https://doi.org/10.1086/505530).
- Collister, A.A., Lahav, O., 2004. ANNz: Estimating Photometric Redshifts Using Artificial Neural Networks. Publications of the ASP 116, 345–351. doi:[10.1086/383254](https://doi.org/10.1086/383254), [arXiv:astro-ph/0311058](https://arxiv.org/abs/astro-ph/0311058).
- Crocce, M., Ross, A.J., Sevilla-Noarbe, I., Gaztanaga, E., Elvin-Poole, J., Avila, S., Alarcon, A., Chan, K.C., Banik, N., Carretero, J., Sanchez, E., Hartley, W.G., Sánchez, C., Giannantonio, T., Rosenfeld, R., Salvador,

- A.I., Garcia-Fernandez, M., García-Bellido, J., Abbott, T.M.C., Abdalla, F.B., Allam, S., Annis, J., Bechtol, K., Benoit-Lévy, A., Bernstein, G.M., Bernstein, R.A., Bertin, E., Brooks, D., Buckley-Geer, E., Rosell, A.C., Kind, M.C., Castander, F.J., Cawthon, R., Cunha, C.E., D’Andrea, C.B., da Costa, L.N., Davis, C., De Vicente, J., Desai, S., Diehl, H.T., Doel, P., Drlica-Wagner, A., Eifler, T.F., Fosalba, P., Frieman, J., García-Bellido, J., Gerdes, D.W., Gruen, D., Gruendl, R.A., Gschwend, J., Gutierrez, G., Hollowood, D., Honscheid, K., Jain, B., James, D.J., Krause, E., Kuehn, K., Kuhlmann, S., Kuropatkin, N., Lahav, O., Lima, M., Maia, M.A.G., Marshall, J.L., Martini, P., Menanteau, F., Miller, C.J., Miquel, R., Nichol, R.C., Percival, W.J., Plazas, A.A., Sako, M., Scarpine, V., Schindler, R., Scolnic, D., Sheldon, E., Smith, M., Smith, R.C., Soares-Santos, M., Sobreira, F., Suchyta, E., Swanson, M.E.C., Tarle, G., Thomas, D., Tucker, D.L., Vikram, V., Walker, A.R., Yanny, B., Zhang, Y., Collaboration, D.E.S., 2018. Dark energy survey year 1 results: galaxy sample for bao measurement. *Monthly Notices of the Royal Astronomical Society* 482, 2807–2822. URL: <https://doi.org/10.1093/mnras/sty2522>, doi:10.1093/mnras/sty2522, arXiv:<https://academic.oup.com/mnras/article-pdf/482/2/2807/26576969/sty2522.pdf>
- Csiszár, I., Shields, P., 2004. Information theory and statistics: A tutorial. *Foundations and Trends® in Communications and Information Theory* 1, 417–528. URL: <http://dx.doi.org/10.1561/0100000004>, doi:10.1561/0100000004.
- Dalmasso, N., Pospisil, T., Lee, A., Izbicki, R., Freeman, P., Malz, A., 2020. Conditional density estimation tools in python and r with applications to photometric redshifts and likelihood-free cosmological inference. *Astronomy and Computing* 30, 100362. URL: <https://www.sciencedirect.com/science/article/pii/S2213133719301313>, doi:<https://doi.org/10.1016/j.ascom.2019.100362>.
- Dawid, A.P., 1984. Present position and potential developments: Some personal views: Statistical theory: The prequential approach. *Journal of the Royal Statistical Society. Series A (General)* 147, 278–292. URL: <http://www.jstor.org/stable/2981683>.
- Dey, B., Newman, J.A., Andrews, B.H., Izbicki, R., Lee, A.B., Zhao, D., Rau, M.M., Malz, A.I., 2021. Re-calibrating photometric redshift probability

distributions using feature-space regression. *Advances in neural information processing systems* URL: <https://par.nsf.gov/biblio/10332320>.

D’Isanto, A., Polsterer, K.L., 2018. Photometric redshift estimation via deep learning. Generalized and pre-classification-less, image based, fully probabilistic redshifts. *Astronomy and Astrophysics* 609, A111. doi:[10.1051/0004-6361/201731326](https://doi.org/10.1051/0004-6361/201731326), [arXiv:1706.02467](https://arxiv.org/abs/1706.02467).

Drlica-Wagner, A., Sevilla-Noarbe, I., Rykoff, E.S., Gruendl, R.A., Yanny, B., Tucker, D.L., Hoyle, B., Rosell, A.C., Bernstein, G.M., Bechtol, K., Becker, M.R., Benoit-Lévy, A., Bertin, E., Kind, M.C., Davis, C., de Vicente, J., Diehl, H.T., Gruen, D., Hartley, W.G., Leistedt, B., Li, T.S., Marshall, J.L., Neilsen, E., Rau, M.M., Sheldon, E., Smith, J., Troxel, M.A., Wyatt, S., Zhang, Y., Abbott, T.M.C., Abdalla, F.B., Allam, S., Banerji, M., Brooks, D., Buckley-Geer, E., Burke, D.L., Capozzi, D., Carretero, J., Cunha, C.E., D’Andrea, C.B., da Costa, L.N., DePoy, D.L., Desai, S., Dietrich, J.P., Doel, P., Evrard, A.E., Neto, A.F., Flaugher, B., Fosalba, P., Frieman, J., García-Bellido, J., Gerdes, D.W., Giannantonio, T., Gschwend, J., Gutierrez, G., Honscheid, K., James, D.J., Jeltama, T., Kuehn, K., Kuhlmann, S., Kuropatkin, N., Lahav, O., Lima, M., Lin, H., Maia, M.A.G., Martini, P., McMahon, R.G., Melchior, P., Menanteau, F., Miquel, R., Nichol, R.C., Ogando, R.L.C., Plazas, A.A., Romer, A.K., Roodman, A., Sanchez, E., Scarpine, V., Schindler, R., Schubnell, M., Smith, M., Smith, R.C., Soares-Santos, M., Sobreira, F., Suchyta, E., Tarle, G., Vikram, V., Walker, A.R., Wechsler, R.H., Zuntz, J., Collaboration), D., 2018. Dark energy survey year 1 results: The photometric data set for cosmology. *The Astrophysical Journal Supplement Series* 235, 33. URL: <https://dx.doi.org/10.3847/1538-4365/aab4f5>, doi:[10.3847/1538-4365/aab4f5](https://doi.org/10.3847/1538-4365/aab4f5).

D’Isanto, A., Polsterer, K. L., 2018. Photometric redshift estimation via deep learning - generalized and pre-classification-less, image based, fully probabilistic redshifts. *A&A* 609, A111. URL: <https://doi.org/10.1051/0004-6361/201731326>, doi:[10.1051/0004-6361/201731326](https://doi.org/10.1051/0004-6361/201731326).

Garcia-Fernandez, M., Sanchez, E., Sevilla-Noarbe, I., Suchyta, E., Huff, E.M., Gaztanaga, E., Aleksić, J., Ponce, R., Castander, F.J., Hoyle, B., Abbott, T.M.C., Abdalla, F.B., Allam, S., Annis, J., Benoit-Lévy, A., Bernstein, G.M., Bertin, E., Brooks, D., Buckley-Geer, E., Burke,

- D.L., Carnero Rosell, A., Carrasco Kind, M., Carretero, J., Crocce, M., Cunha, C.E., D’Andrea, C.B., da Costa, L.N., DePoy, D.L., Desai, S., Diehl, H.T., Eifler, T.F., Evrard, A.E., Fernandez, E., Flaugh, B., Fosalba, P., Frieman, J., García-Bellido, J., Gerdes, D.W., Gianantonio, T., Gruen, D., Gruendl, R.A., Gschwend, J., Gutierrez, G., James, D.J., Jarvis, M., Kirk, D., Krause, E., Kuehn, K., Kuropatkin, N., Lahav, O., Lima, M., MacCrann, N., Maia, M.A.G., March, M., Marshall, J.L., Melchior, P., Miquel, R., Mohr, J.J., Plazas, A.A., Romer, A.K., Roodman, A., Rykoff, E.S., Scarpine, V., Schubnell, M., Smith, R.C., Soares-Santos, M., Sobreira, F., Tarle, G., Thomas, D., Walker, A.R., Wester, W., Collaboration), T.D., 2018. Weak lensing magnification in the dark energy survey science verification data. *Monthly Notices of the Royal Astronomical Society* 476, 1071–1085. URL: <https://doi.org/10.1093/mnras/sty282>, doi:10.1093/mnras/sty282, arXiv:<https://academic.oup.com/mnras/article-pdf/476/1/1071/24239965/sty282.pdf>.
- Gerdes, D.W., Sypniewski, A.J., McKay, T.A., Hao, J., Weis, M.R., Wechsler, R.H., Busha, M.T., 2010. ArborZ: Photometric Redshifts Using Boosted Decision Trees. *Astrophysical Journal* 715, 823–832. doi:10.1088/0004-637X/715/2/823, arXiv:0908.4085.
- Goodfellow, I., Bengio, Y., Courville, A., 2016. *Deep Learning*. MIT Press. <http://www.deeplearningbook.org>.
- Goodfellow, I.J., Pouget-Abadie, J., Mirza, M., Xu, B., Warde-Farley, D., Ozair, S., Courville, A., Bengio, Y., 2014. Generative adversarial nets, in: *Proceedings of the 27th International Conference on Neural Information Processing Systems - Volume 2*, MIT Press, Cambridge, MA, USA. p. 2672–2680.
- Graham, M.L., Connolly, A.J., Ivezić, Ž., Schmidt, S.J., Jones, R.L., Jurić, M., Daniel, S.F., Yoachim, P., 2018. Photometric Redshifts with the LSST: Evaluating Survey Observing Strategies. *Astronomical Journal* 155, 1. doi:10.3847/1538-3881/aa99d4, arXiv:1706.09507.
- Hermans, J., Begy, V., Louppe, G., 2020. Likelihood-free mcmc with amortized approximate ratio estimators. URL: <https://arxiv.org/abs/1903.04057>, arXiv:1903.04057.

- Hiriart-Urruty, J.B., Lemaréchal, C., 2001. Fundamentals of Convex Analysis / J.B. Hiriart-Urruty, C. Lemaréchal. doi:[10.1007/978-3-642-56468-0](https://doi.org/10.1007/978-3-642-56468-0).
- Hoyle, B., 2016. Measuring photometric redshifts using galaxy images and deep neural networks. *Astronomy and Computing* 16, 34–40. URL: <https://www.sciencedirect.com/science/article/pii/S221313371630021X>, doi:<https://doi.org/10.1016/j.ascom.2016.03.006>.
- Karras, T., Aila, T., Laine, S., Lehtinen, J., 2018. Progressive growing of GANs for improved quality, stability, and variation, in: International Conference on Learning Representations. URL: <https://openreview.net/forum?id=Hk99zCeAb>.
- Kullback, S., Leibler, R.A., 1951. On Information and Sufficiency. *The Annals of Mathematical Statistics* 22, 79 – 86. URL: <https://doi.org/10.1214/aoms/1177729694>, doi:[10.1214/aoms/1177729694](https://doi.org/10.1214/aoms/1177729694).
- Laur, J., Tempel, E., Tamm, A., Kipper, R., Liivamägi, L.J., Hernán-Caballero, A., Muru, M.M., Chaves-Montero, J., Díaz-García, L.A., Turner, S., Tuvikene, T., Queiroz, C., Bom, C.R., Fernández-Ontiveros, J.A., González Delgado, R.M., Civera, T., Abramo, R., Alcaniz, J., Benítez, N., Bonoli, S., Carneiro, S., Cenarro, J., Cristóbal-Hornillos, D., Dupke, R., Ederoclite, A., López-Sanjuan, C., Marín-Franch, A., de Oliveira, C.M., Moles, M., Sodr e, L., Taylor, K., Varela, J., Vázquez Rami o, H., 2022. TOPz: Photometric redshifts for J-PAS. *Astronomy and Astrophysics* 668, A8. doi:[10.1051/0004-6361/202243881](https://doi.org/10.1051/0004-6361/202243881), [arXiv:2209.01040](https://arxiv.org/abs/2209.01040).
- Leistedt, B., Hogg, D.W., Wechsler, R.H., DeRose, J., 2019. Hierarchical modeling and statistical calibration for photometric redshifts. *The Astrophysical Journal* 881, 80. URL: <https://dx.doi.org/10.3847/1538-4357/ab2d29>, doi:[10.3847/1538-4357/ab2d29](https://doi.org/10.3847/1538-4357/ab2d29).
- Liese, F., Vajda, I., 2006. On divergences and informations in statistics and information theory. *IEEE Transactions on Information Theory* 52, 4394–4412. doi:[10.1109/TIT.2006.881731](https://doi.org/10.1109/TIT.2006.881731).
- Lima, E., Sodr e, L., Bom, C., Teixeira, G., Nakazono, L., Buzzo, M., Queiroz, C., Herpich, F., Castellon, J.N., Dantas, M., Dors,

- O., de Souza, R.T., Akras, S., Jiménez-Teja, Y., Kanaan, A., Ribeiro, T., Schoennell, W., 2022. Photometric redshifts for the s-plus survey: Is machine learning up to the task? *Astronomy and Computing* 38, 100510. URL: <https://www.sciencedirect.com/science/article/pii/S2213133721000640>, doi:<https://doi.org/10.1016/j.ascom.2021.100510>.
- Lu, J., Luo, Z., Chen, Z., Fu, L., Du, W., Gong, Y., Li, Y., Meng, X.M., Tang, Z., Zhang, S., Shu, C., Zhou, X., Fan, Z., 2023. Estimating photometric redshift from mock flux for csst survey by using weighted random forest. *Monthly Notices of the Royal Astronomical Society* 527, 12140–12153. URL: <https://doi.org/10.1093/mnras/stad3976>, doi:[10.1093/mnras/stad3976](https://doi.org/10.1093/mnras/stad3976), arXiv:<https://academic.oup.com/mnras/article-pdf/527/4/12140/55462380/stad3976.pdf>
- Luo, Z., Li, Y., Lu, J., Chen, Z., Fu, L., Zhang, S., Xiao, H., Du, W., Gong, Y., Shu, C., Ma, W., Meng, X., Zhou, X., Fan, Z., 2024. Photometric redshift estimation for CSST survey with LSTM neural networks. *Monthly Notices of the Royal Astronomical Society* 535, 1844–1855. doi:[10.1093/mnras/stae2446](https://doi.org/10.1093/mnras/stae2446), arXiv:[2410.19402](https://arxiv.org/abs/2410.19402).
- Mahmud Pathi, I., Soo, J.Y.H., Jie Wee, M., Nadhilah Zakaria, S., Azwin Ismail, N., Baugh, C.M., Manzoni, G., Gaztanaga, E., Castander, F.J., Eriksen, M., Carretero, J., Fernandez, E., Garcia-Bellido, J., Miquel, R., Padilla, C., Renard, P., Sanchez, E., Sevilla-Noarbe, I., Tallada-Crespí, P., 2024. ANNZ+: an enhanced photometric redshift estimation algorithm with applications on the PAU Survey. arXiv e-prints , arXiv:2409.09981doi:[10.48550/arXiv.2409.09981](https://doi.org/10.48550/arXiv.2409.09981), arXiv:[2409.09981](https://arxiv.org/abs/2409.09981).
- McLachlan, G.J., Lee, S.X., Rathnayake, S.I., 2019. Finite mixture models. *Annual Review of Statistics and Its Application* 6, 355–378. URL: <https://www.annualreviews.org/content/journals/10.1146/annurev-statistics-031017-100325>, doi:<https://doi.org/10.1146/annurev-statistics-031017-100325>.
- Mirza, M., Osindero, S., 2014. Conditional Generative Adversarial Nets. arXiv e-prints , arXiv:1411.1784doi:[10.48550/arXiv.1411.1784](https://doi.org/10.48550/arXiv.1411.1784), arXiv:[1411.1784](https://arxiv.org/abs/1411.1784).

- Mucesh, S., Hartley, W.G., Palmese, A., Lahav, O., Whiteway, L., Bluck, A.F.L., Alarcon, A., Amon, A., Bechtol, K., Bernstein, G.M., Carnero Rosell, A., Carrasco Kind, M., Choi, A., Eckert, K., Everett, S., Gruen, D., Gruendl, R.A., Harrison, I., Huff, E.M., Kuropatkin, N., Sevilla-Noarbe, I., Sheldon, E., Yanny, B., Aguena, M., Allam, S., Bacon, D., Bertin, E., Bhargava, S., Brooks, D., Carretero, J., Castander, F.J., Conselice, C., Costanzi, M., Crocce, M., da Costa, L.N., Pereira, M.E.S., De Vicente, J., Desai, S., Diehl, H.T., Drlica-Wagner, A., Evrard, A.E., Ferrero, I., Flaugher, B., Fosalba, P., Frieman, J., García-Bellido, J., Gaztanaga, E., Gerdes, D.W., Gschwend, J., Gutierrez, G., Hinton, S.R., Hollowood, D.L., Honscheid, K., James, D.J., Kuehn, K., Lima, M., Lin, H., Maia, M.A.G., Melchior, P., Menanteau, F., Miquel, R., Morgan, R., Paz-Chinchón, F., Plazas, A.A., Sanchez, E., Scarpine, V., Schubnell, M., Serrano, S., Smith, M., Suchyta, E., Tarle, G., Thomas, D., To, C., Varga, T.N., Wilkinson, R.D., Collaboration), D., 2021. A machine learning approach to galaxy properties: joint redshift–stellar mass probability distributions with random forest. *Monthly Notices of the Royal Astronomical Society* 502, 2770–2786. URL: <https://doi.org/10.1093/mnras/stab164>, doi:10.1093/mnras/stab164, arXiv:<https://academic.oup.com/mnras/article-pdf/502/2/2770/38831474/stab164.pdf>
- Newman, J.A., Gruen, D., 2022. Photometric Redshifts for Next-Generation Surveys. *Annual Review of Astronomy and Astrophysics* 60, 363–414. doi:10.1146/annurev-astro-032122-014611, arXiv:2206.13633.
- Nguyen, X., Wainwright, M.J., Jordan, M., 2007. Estimating divergence functionals and the likelihood ratio by penalized convex risk minimization, in: Platt, J., Koller, D., Singer, Y., Roweis, S. (Eds.), *Advances in Neural Information Processing Systems*, Curran Associates, Inc. URL: https://proceedings.neurips.cc/paper_files/paper/2007/file/72da7fd6d1302c0a159f6436d01e9eb0-Paper.pdf.
- Nowozin, S., Cseke, B., Tomioka, R., 2016. f-gan: Training generative neural samplers using variational divergence minimization, in: Lee, D., Sugiyama, M., Luxburg, U., Guyon, I., Garnett, R. (Eds.), *Advances in Neural Information Processing Systems*, Curran Associates, Inc. URL: https://proceedings.neurips.cc/paper_files/paper/2016/file/cedebb6e872f539bef8c3f919874e9d7-Paper.pdf.

- Paszke, A., Gross, S., Massa, F., Lerer, A., Bradbury, J., Chanan, G., Killeen, T., Lin, Z., Gimelshein, N., Antiga, L., Desmaison, A., Köpf, A., Yang, E., DeVito, Z., Raison, M., Tejani, A., Chilamkurthy, S., Steiner, B., Fang, L., Bai, J., Chintala, S., 2019. PyTorch: An Imperative Style, High-Performance Deep Learning Library. arXiv e-prints , arXiv:1912.01703doi:10.48550/arXiv.1912.01703, arXiv:1912.01703.
- Pedregosa, F., Varoquaux, G., Gramfort, A., Michel, V., Thirion, B., Grisel, O., Blondel, M., Müller, A., Nothman, J., Louppe, G., Prettenhofer, P., Weiss, R., Dubourg, V., Vanderplas, J., Passos, A., Cournapeau, D., Brucher, M., Perrot, M., Duchesnay, É., 2011. Scikit-learn: Machine Learning in Python. Journal of Machine Learning Research 12, 2825–2830. doi:10.48550/arXiv.1201.0490, arXiv:1201.0490.
- Polsterer, K.L., D’Isanto, A., Gieseke, F., 2016. Uncertain photometric redshifts. URL: <https://arxiv.org/abs/1608.08016>, arXiv:1608.08016.
- Rau, M.M., Seitz, S., Brimiouille, F., Frank, E., Friedrich, O., Gruen, D., Hoyle, B., 2015. Accurate photometric redshift probability density estimation – method comparison and application. Monthly Notices of the Royal Astronomical Society 452, 3710–3725. URL: <https://doi.org/10.1093/mnras/stv1567>, doi:10.1093/mnras/stv1567, arXiv:<https://academic.oup.com/mnras/article-pdf/452/4/3710/18241297/stv1567.pdf>
- Reid, M.D., Williamson, R.C., 2011. Information, divergence and risk for binary experiments. Journal of Machine Learning Research 12, 731–817. URL: <http://jmlr.org/papers/v12/reid11a.html>.
- Sadeh, I., Abdalla, F.B., Lahav, O., 2016. ANNz2: Photometric Redshift and Probability Distribution Function Estimation using Machine Learning. Publications of the ASP 128, 104502. doi:10.1088/1538-3873/128/968/104502, arXiv:1507.00490.
- Salvato, M., Ilbert, O., Hoyle, B., 2019. The many flavours of photometric redshifts. Nature Astronomy 3, 212–222. doi:10.1038/s41550-018-0478-0, arXiv:1805.12574.
- Schaap, W.E., van de Weygaert, R., 2000. Continuous fields and discrete samples: reconstruction through Delaunay tessellations. Astronomy

- and *Astrophysics* 363, L29–L32. doi:[10.48550/arXiv.astro-ph/0011007](https://doi.org/10.48550/arXiv.astro-ph/0011007), [arXiv:astro-ph/0011007](https://arxiv.org/abs/astro-ph/0011007).
- Schuldt, S., Suyu, S.H., Cañameras, R., Taubenberger, S., Meinhardt, T., Leal-Taixé, L., Hsieh, B.C., 2021. Photometric redshift estimation with a convolutional neural network: NetZ. *Astronomy and Astrophysics* 651, A55. doi:[10.1051/0004-6361/202039945](https://doi.org/10.1051/0004-6361/202039945), [arXiv:2011.12312](https://arxiv.org/abs/2011.12312).
- Song, J., Ermon, S., 2020. Bridging the gap between f-GANs and Wasserstein GANs, in: III, H.D., Singh, A. (Eds.), *Proceedings of the 37th International Conference on Machine Learning*, PMLR. pp. 9078–9087. URL: <https://proceedings.mlr.press/v119/song20a.html>.
- Sánchez, C., Carrasco Kind, M., Lin, H., Miquel, R., Abdalla, F.B., Amara, A., Banerji, M., Bonnett, C., Brunner, R., Capozzi, D., Carnero, A., Castander, F.J., da Costa, L.A.N., Cunha, C., Fausti, A., Gerdes, D., Greisel, N., Gschwend, J., Hartley, W., Jouvel, S., Lahav, O., Lima, M., Maia, M.A.G., Martí, P., Ogando, R.L.C., Ostrovski, F., Pellegrini, P., Rau, M.M., Sadeh, I., Seitz, S., Sevilla-Noarbe, I., Sypniewski, A., de Vicente, J., Abbot, T., Allam, S.S., Atlee, D., Bernstein, G., Bernstein, J.P., Buckley-Geer, E., Burke, D., Childress, M.J., Davis, T., DePoy, D.L., Dey, A., Desai, S., Diehl, H.T., Doel, P., Estrada, J., Evrard, A., Fernández, E., Finley, D., Flaugh, B., Frieman, J., Gaztanaga, E., Glazebrook, K., Honscheid, K., Kim, A., Kuehn, K., Kuropatkin, N., Lidman, C., Makler, M., Marshall, J.L., Nichol, R.C., Roodman, A., Sánchez, E., Santiago, B.X., Sako, M., Scalzo, R., Smith, R.C., Swanson, M.E.C., Tarle, G., Thomas, D., Tucker, D.L., Uddin, S.A., Valdés, F., Walker, A., Yuan, F., Zuntz, J., 2014. Photometric redshift analysis in the dark energy survey science verification data. *Monthly Notices of the Royal Astronomical Society* 445, 1482–1506. URL: <https://doi.org/10.1093/mnras/stu1836>, doi:[10.1093/mnras/stu1836](https://doi.org/10.1093/mnras/stu1836), [arXiv:https://academic.oup.com/mnras/article-pdf/445/2/1482/18197851/stu1836.pdf](https://academic.oup.com/mnras/article-pdf/445/2/1482/18197851/stu1836.pdf).
- Teixeira, G., Bom, C., Santana-Silva, L., Fraga, B., Darc, P., Teixeira, R., Wu, J., Ferguson, P., Martínez-Vázquez, C., Riley, A., Drlica-Wagner, A., Choi, Y., Mutlu-Pakdil, B., Pace, A., Sakowska, J., Stringfellow, G., 2024. Photometric redshifts probability density estimation from recurrent neural networks in the decam local volume exploration survey data release 2. *Astronomy and Computing* 49, 100886. URL: <https://www.sciencedirect.com>.

[com/science/article/pii/S221313372400101X](https://doi.org/10.1016/j.ascom.2024.100886), doi:<https://doi.org/10.1016/j.ascom.2024.100886>.

Yu, G., Sapiro, G., Mallat, S., 2012. Solving inverse problems with piecewise linear estimators: From gaussian mixture models to structured sparsity. *IEEE Transactions on Image Processing* 21, 2481–2499. doi:[10.1109/TIP.2011.2176743](https://doi.org/10.1109/TIP.2011.2176743).